Oscillating Coulomb chain in a storage ring

H. Okamoto, Y. Yuri, and K. Okabe

Department of Quantum Matter, Graduate School of Advanced Sciences of Matter, Hiroshima University, 1-3-1 Kagamiyama,
Higashi-Hiroshima 739-8530, Japan

The dynamic behavior of a bunched one-dimensional crystalline beam is studied theoretically. It is shown that, owing to the existence of momentum dispersion, a Coulomb chain traveling in a storage ring performs a complex periodic oscillation whenever it is exposed to a longitudinal radio-frequency force. The equations of motion are derived to predict the oscillation pattern in an arbitrary lattice structure. The validity of the present theory is confirmed through multiparticle simulations. Various features of an oscillating string beam, such as the lattice-parameter dependence of the orbit, the stability, and critical line density, etc., are also discussed.

I. INTRODUCTION

The first application of the laser-cooling technique to a relativistic ion beam was carried out in 1990 at the Heidelberg TSR storage ring [1]. It was experimentally demonstrated that the longitudinal motion of a fast stored beam is well controllable by the photon pressure. This seminal work, followed by another important experiment at the ASTRID storage ring of Aarhus University [2], opened up a possibility for reaching the ultimate state of a charged-particle beam. In fact, the Doppler limit of laser cooling is typically in a milli-Kelvin range or even below, several orders of magnitude lower than the beam temperature achievable with other cooling methods [3]. If the Doppler limit is reached in all three degrees of freedom, the beam will then be Coulomb crystallized as theoretically suggested by Schiffer and co-workers [4].

After the experiments at TSR and ASTRID, theoretical and experimental studies of beam crystallization became more active, and many new insights have been gained concerning the dynamics of highly space-charge-dominated beams [3,5–10]. Nevertheless, nobody has succeeded so far in realizing beam crystallization in a storage ring, although circulating Coulomb crystals were recently obtained in a compact ring-shaped Paul trap system called PALLAS [11]. To our current knowledge, there are three primary reasons why crystallizing a relativistic beam is so difficult:

(a) it is impossible for existing cooler storage rings to meet the stability requirements of a crystalline state;

(b) laser-cooling force directly operates only in the longitudinal direction of beam motion;

(c) any storage-ring lattice contains dipole magnets that inevitably yield momentum dispersion.

At sufficiently high line density, the resultant crystalline structure is multidimensional; the two-dimensional zigzag or a three-dimensional shell configuration is formed [12]. We, however, need a special *tapered* force to stabilize such a crystalline beam with a finite transverse dimension, whereas no practical method has been established so far for tapering the photon pressure [7,13]. Further, as mentioned above in the item (a), the transverse betatron motion eventually becomes unstable unless the lattice of the ring has been properly designed so as to prevent the occurrence of collective instability during a cooling process [14]. These facts suggest that it is almost hopeless at present to crystallize a fast stored beam of high line density. By contrast, the production of a one-dimensional string crystal may be possible. Since its heating rate due to Coulomb collisions is rather low [7], it would be relatively easy to overcome the instability [15]. As a matter of fact, in the middle 1990s, a sudden jump of the Schottky signal from highly charged ions, similar to that reported from Russian researchers in the late 1970s [16], was observed in electron cooling experiments at the ESR ring of GSI [17]. An analogous phenomenon was also confirmed at CRYRING of Manne Siegbahn Laboratory [18]. These anomalies observed at very low line density are thought to be a sign of the phase transition to a sort of liquid state. A theoretical investigation has concluded that the beam established a stringlike order where the individual ions still execute transverse oscillations but cannot pass each other longitudinally [19].

Needless to say, understanding the nature of a one-dimensional crystalline beam is practically very important; it would be impossible to realize other crystal configurations if the string cannot be formed. All particles forming a *coasting* Coulomb chain sit exactly on the design closed orbit of the storage ring. In this simple case, nothing physically interesting takes place as the beam is completely frozen in the rest frame. However, once a longitudinal radio-frequency (rf) field is switched on, even a string crystalline beam comes to exhibit a complicated dynamic behavior [20]. Since the rf force induces finite energy difference among particles, even an ideal string can no longer stay on the design orbit but is forced to oscillate horizontally due to the existence of momentum dispersion. In this paper, we extensively study the dynamics of *bunched* Coulomb chains in a storage ring. We first derive in Sec. II a set of equations that govern the motion of a bunched string. The validity of the proposed equations is tested in Sec. III through multiparticle simulations. Section IV is devoted to describing various unique features of oscillating crystalline beams. In particular, we discuss the lattice-parameter dependence of string motion, the stability and equilibrium temperature of ground states, etc. Finally, the present results are summarized in Sec. V.

II. EQUATION OF MOTION OF A BUNCHED COULOMB CHAIN

Consider a storage ring composed of dipole and quadrupole magnets. We further put one or more identical rf cavities that produce longitudinal electric force. Charged particles traveling in this system obey the following canonical equations of motion in the rest frame [21]:

$$x' = p_x, \tag{1}$$

$$p_x' = \frac{\gamma}{\rho} p_z - K_x(\tau) x - \frac{r_p}{\beta^2 \gamma^2} \frac{\partial U_c(x,z)}{\partial x}, \tag{2}$$

$$z' = p_z - \frac{\gamma}{\rho} x, \tag{3}$$

$$p_z' = -\frac{r_p}{\beta^2 \gamma^2} \frac{\partial U_c(x,z)}{\partial z} - \frac{q}{m_0(\beta \gamma c)^2} \frac{\partial U_{rf}(z;\tau)}{\partial z}, \tag{4}$$

where r_p, q, and m_0 are, respectively, the classical radius, total charge, and rest mass of the particle, c is the speed of light, β and γ are the Lorentz factors, ρ is the local curvature of the design orbit, K_x is the horizontal focusing function, the scaled rf potential denoted by U_{rf} is uniform in the transverse directions, the independent variable has been defined as $\tau = \beta \gamma c t$ with t being the proper time, and the prime stands for differentiation with respect to τ. Note that the vertical degree of freedom has been ignored because in this section, we concentrate upon the behavior of an ideal one-dimensional crystalline beam. The scaled Coulomb potential is then given by

$$U_c(x,z) = \sum_j \frac{1}{\sqrt{(x_j - x)^2 + (z_j - z)^2}}, \tag{5}$$

where x_j and z_j are the spatial coordinates of jth particle. Since the rf force has been introduced only for the purpose of beam bunching, the synchronous phase is always chosen to be zero. In this case, the synchronous ion located at the center of the string crystal passes through a cavity at a moment when the rf electric field switches from decelerating phase to accelerating phase. We also assume, for the sake of simplicity, that the cavities are symmetrically arranged; i.e., $U_{rf}(z) = U_{rf}(z+L)$, where L is the distance from one cavity to the next. If the ring has only one cavity, L, of course, agrees with the total length of the design closed orbit.

In any crystalline ground state, all particles are precisely aligned in the transverse phase space, which means that the emittance is equal to zero [10]. Since a string crystal has a linear configuration even in real space, we can express the coordinates of individual particles in the form

$$x_j = C_j D_x(\tau), \quad z_j = C_j D_z(\tau), \tag{6}$$

where C_j is a particle-dependent constant, while D_x and D_z are periodic functions universal among all particles. Specifically, the value of D_z cannot cross zero; otherwise, the string configuration is destroyed. It is straightforward to show that

these particles actually form a straight line in an arbitrary two-dimensional space. An analogous expression applies to multidimensional coasting crystalline beams as well [10].

Let us now keep our eyes on, say, nth particle. We drop the subscript n, simply writing the canonical variables as (x,z,p_x,p_z). If this is not the synchronous particle, the longitudinal momentum p_z suddenly jumps every time when it goes across a cavity. Because of the periodic nature of the string motion, each jump will occur symmetrically; if the value of p_z were $-p_0$ just before a cavity, it would jump to $+p_0$ after the interaction with the rf field. Further, the variation of p_z is expected to be smooth and simple in-between two adjacent cavities since no longitudinal artificial force is there. It is, therefore, reasonable to assume

$$p_z = C_n \alpha(\tau) \left(\frac{\tau}{L} - \frac{1}{2} \right), \tag{7}$$

where the origin of τ has been taken at the cavity position. $\alpha(\tau)$ is a τ-dependent function represented as $\alpha(\tau) = \bar{\alpha}[1 + \eta(\tau)]$, where $\bar{\alpha}$ denotes the average value of $\alpha(\tau)$, and $\eta(\tau)$ is a periodic modulation satisfying $|\eta| \ll 1$ and $L|\eta'| \ll 1$. The total amount of a momentum jump at each cavity is clearly $C_n \bar{\alpha}$ that can be related to the energy gain of the particle. Assuming a usual sinusoidal rf potential with the harmonic number of h and the amplitude of V_0, we obtain the approximate relation $C_n \bar{\alpha} \approx [q/m_0(\beta \gamma c)^2] V_0 \sin[(2\pi h \gamma/N_{sp})(C_n D_z(0)/L)]$ where N_{sp} is the lattice periodicity of the ring. This relation gives

$$\bar{\alpha} \approx \frac{(2\pi \nu_z)^2}{|\xi_0| N_{sp}} \frac{D_z(0)}{L}, \tag{8}$$

where ξ_0 is the phase slip factor and $\nu_z^2 \equiv hq|\xi_0|V_0/2\pi m_0 \gamma(\beta c)^2$. The parameter ν_z directly corresponds to the synchrotron tune provided that $\nu_z \ll 1$. Substituting Eq. (7) into Eq. (4), we have the equation relevant in the region between two neighboring cavities:

$$C_n \bar{\alpha} \eta' \left(\frac{\tau}{L} - \frac{1}{2} \right) + C_n \frac{\bar{\alpha}}{L}(1+\eta) = -\frac{r_p}{\beta^2 \gamma^2} S_n \frac{D_z}{(D_x^2 + D_z^2)^{3/2}}, \tag{9}$$

where $S_n = \sum_{j \neq n}^{j} (C_j - C_n)/|C_j - C_n|^3$. Since $|\eta| \ll 1$ and $L|\eta'| \ll 1$, Eq. (9) can be approximated as $C_n \bar{\alpha}/L \approx -(r_p/\beta^2 \gamma^2) S_n D_z/(D_x^2 + D_z^2)^{3/2}$. This equation indicates that D_z is nearly constant, because the longitudinal extent of a string crystal is generally much greater than the horizontal extent, i.e., $|D_x/D_z| \ll 1$. From Eqs. (1) and (2) together with Eqs. (5)–(9), we eventually find

$$D_x'' + K_x(\tau) D_x = \frac{1}{N_{sp}L} \frac{(2\pi \nu_z)^2}{|\xi_0|} \left[\frac{D_x}{L} + \left(\frac{\tau}{L} - \frac{1}{2} \right) \frac{\gamma D_z}{\rho} \right], \tag{10}$$

where we have replaced $D_z(0)$ by $D_z(\tau)$ recalling that $D_z(\tau) \approx$ const as pointed out above. Similarly, Eq. (3) leads to

TABLE I. Simulation parameters.

Ion species	^{24}Mg$^+$
Total kinetic energy	1 MeV
Lattice	TARN II
Superperiodicity	6 (without cavities)
Circumference	77.7 m
Bare betatron tunes (ν_x, ν_y)	Case I (2.10, 2.10) and Case II (2.30, 2.30)
Transition γ	2.255 (Case I), 2.444 (Case II)
Phase slip factor	-0.803 (Case I), -0.832 (Case II)
rf harmonic number	1000
rf voltage amplitude	<150 V
Bare synchrotron tune	$0.01 \sim 0.1$

$$D_z' = \frac{1}{N_{sp}L}\frac{(2\pi\nu_z)^2}{|\xi_0|}\left(\frac{\tau}{L}-\frac{1}{2}\right)D_z - \frac{\gamma}{\rho}D_x. \qquad (11)$$

In these equations, the independent variable τ varies in the region $0 < \tau/L < 1$. The basic properties of a bunched Coulomb chain can be predicted by solving Eqs. (10) and (11).

III. SIMULATION RESULTS

In order to test whether Eqs. (10) and (11) can well reproduce the motion of a bunched Coulomb chain, systematic multiparticle simulations were performed. In our code, we numerically iterate the three-dimensional equations of particle motion, incorporating the characteristics of an actual storage ring like bending and straight sections, and alternating-gradient focusing. Since the number of particles in a single bunch is not too large, real particles are employed to evaluate the exact Coulomb interactions among them. As to the lattice structure, we chose the design parameters of the cooler storage ring TARN II [22]. The lattice of TARN II, whose circumference is 77.7 m, has sixfold symmetry. The betatron phase advance per single superperiod can be reduced to near 90° or even less, so that the stability condition of crystalline beams is fulfilled [7]. The ion species considered here is ^{24}Mg$^+$ that has been often used in past laser-cooling experiments. The main simulation parameters are listed in Table I.

In this section, we take the case-I lattice in which the betatron tunes have been adjusted to $(\nu_x, \nu_y) = (2.10, 2.10)$. An rf cavity is installed in one of the six straight sections to bunch a 1 MeV ^{24}Mg$^+$-ion beam. The amplitude of the rf voltage is set at 38.65 V corresponding to the single-particle synchrotron tune of 0.05. In a test simulation, we initially distributed 27 particles at random positions in phase space and, then, applied a three-dimensional modest dissipative force to cool them. To save the computing time, the simplest cooling model was adopted; we damped the transverse and longitudinal momenta of all ions once in a turn, using the linear transformation

$$(p_\ell)_{\text{out}} - (p_\ell)_{\text{in}} = -f_\ell (p_\ell)_{\text{in}} \quad (\ell = x, y, z), \qquad (12)$$

where $(p_\ell)_{\text{in}}$ and $(p_\ell)_{\text{out}}$ are the canonical momenta before and after the cooling point, and f_ℓ is the cooling strength.

Under these conditions, the beam finally reached an ordered state as shown in Fig. 1 where the real-space configuration observed at a certain location of TARN II has been depicted. Each small circle stands for a single ^{24}Mg$^+$ ion. We confirm that the ions are horizontally deviated from the design orbit due to the momentum dispersion. They execute periodic oscillations in the horizontal plane, keeping the linear configuration as a whole. On the other hand, the beam profile in the vertical plane was almost static.

Figure 2 demonstrates the trajectories of three ions arbitrarily picked from the crystal in Fig. 1. It is evident from the last panel that the assumption in Eq. (7) is adequate. The cavity is sitting at the coordinate $\tau = 25.9$ m where the sharp momentum jump has occurred. Scaling these single-particle trajectories via Eq. (6), we obtain Fig. 3. The three orbits, plotted in broken lines, have now completely overlapped with each other. The solid lines represent the stationary so-
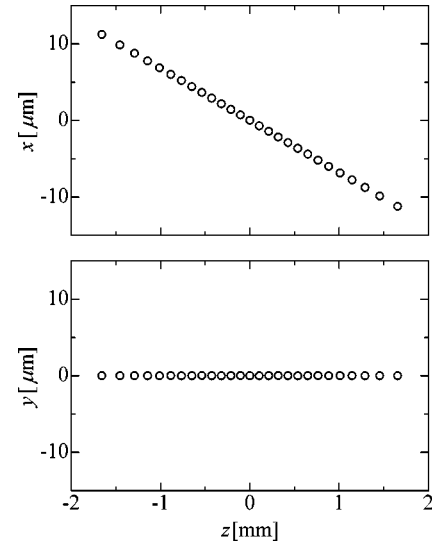
FIG. 1. Spatial configuration of a bunched "string" crystalline beam obtained from a multiparticle simulation. The TARN II lattice containing a single rf cavity has been taken into account. The horizontal and vertical betatron tunes are $(\nu_x, \nu_y) = (2.10, 2.10)$, and the synchrotron tune is 0.05 in the absence of space charge. Each circle represents a single ^{24}Mg$^+$ ion traveling at the kinetic energy of 1 MeV. The friction coefficients have been chosen to be $f_x = f_y = 0.01$ and $f_z = 0.11$.
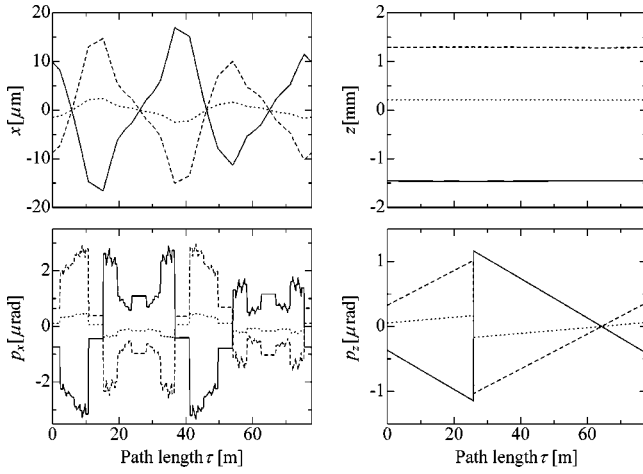
FIG. 2. Single-particle orbits in a bunched string crystalline beam. The trajectories of three ^{24}Mg$^+$ ions arbitrarily selected from the beam in Fig. 1 have been plotted.

lution to Eqs. (10) and (11), which indicates that the present theory explains the multiparticle simulation result fairly well. It is also recognized that all particles are on the design beam line when passing through the cavity. Since the rf force longitudinally compresses the beam, the bunch length should be maximum at the cavity. However, the change of D_z was generally negligible according to our simulations. This implies that the total length of the Coulomb chain is nearly constant all around the ring, because the ratio $|D_x/D_z|$ is always small.
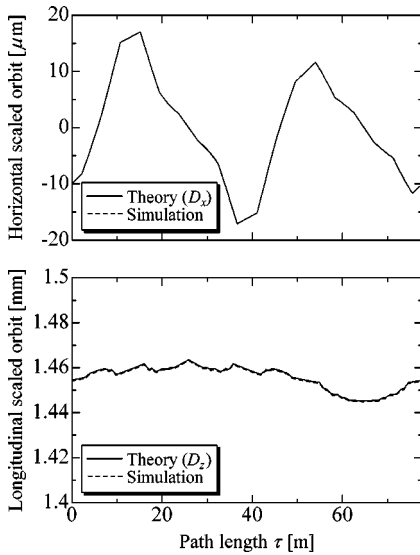
FIG. 3. Horizontal and longitudinal scaled orbits. The three trajectories shown in Fig. 2 have been scaled according to Eq. (6). The values of the scaling parameters used here are $C_1 = -1.00$, $C_2 = 1.13$, and $C_3 = 6.88$. The scaled orbits plotted in broken lines have completely overlapped with each other. The solid lines in both pictures show the orbit functions D_x and D_z evaluated from Eqs. (10) and (11). We see that the theoretical prediction is in excellent agreement with the multiparticle simulation result.
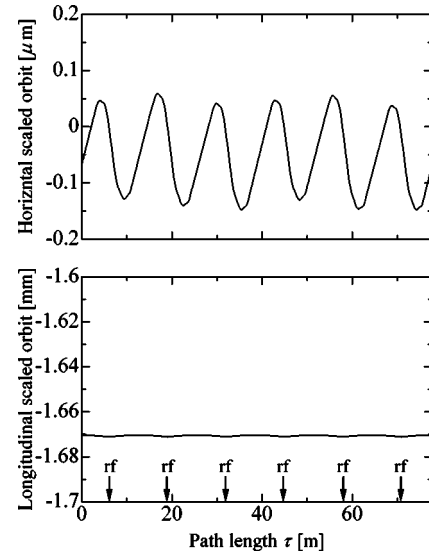
FIG. 4. Horizontal and longitudinal scaled orbits obtained from a multiparticle simulation. An rf cavity is installed in each lattice period. Other conditions are identical to those assumed in Fig. 1. Since the ring now contains six cavities, the rf voltage has been reduced to 6.44 V in order to maintain the bare synchrotron tune at 0.05. The small arrows in the lower picture indicate the longitudinal positions where the cavities are located.

IV. CHARACTERISTICS OF OSCILLATING COULOMB CHAINS

A. Lattice dependence

In the case-I lattice with a single rf cavity, a string crystalline beam oscillates about the design closed orbit two times per turn regardless of the synchrotron tune and cavity position. Note, however, that the number of rf cavities plays an essential role in the orbit equations (10) and (11); it has actually determined the oscillation period of the stationary solution. Since the energy jump occurs only at the cavity position, the period of the longitudinal motion is inevitably equal to the ring circumference as long as the lattice contains only one cavity. The horizontal motion must then have the same oscillation period despite the fact that the transverse focusing force repeats an identical variation pattern six times around the ring.

A question is what happens if we put an rf cavity in every lattice period so that the ring recovers strict sixfold symmetry. Figure 4 shows an example of the scaled orbit when six cavities are set at intervals of 12.95 m. Other conditions are the same as those assumed in the previous figures (while the rf voltage has been reduced to 6.44 V in order to keep the bare synchrotron tune at 0.05). Unlike the result in Fig. 3, the particle trajectory has exhibited approximate sixfold symmetry. The weak symmetry breakdown comes from the cooling force; we can verify that oscillation patterns within the six lattice periods perfectly agree with each other if six cooling sections are symmetrically inserted in the ring.

We have also confirmed numerically that the scaled orbit strongly depends on the positions of the rf cavities. To illustrate this, let us shift all the cavities in Fig. 4 by 3.1 m along the beam line. The orbit is then completely altered as dis-
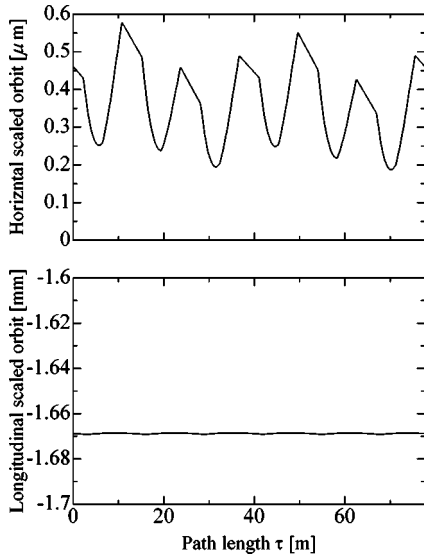
FIG. 5. Horizontal and longitudinal scaled orbits obtained from a multiparticle simulation. We have assumed exactly the same lattice parameters as used in Fig. 4, except for the locations of the six rf cavities.

played in Fig. 5. Each ion now executes a small periodic oscillation not about the design orbit but about a certain horizontal coordinate. The maximum value of D_x calculated from Eqs. (10) and (11) has been plotted in Fig. 6 as a function of the cavity position. In this plot, we have considered six cooling sections in order for the particle orbit to achieve exact sixfold symmetry. Only when a cavity is located within the shaded regions in Fig. 6, the orbits of individual ions cross zero just like the case in Fig. 4. Outside this area, the oscillation pattern becomes similar to that in Fig. 5.

B. Stability

Without the rf force, it will always be possible to construct a one-dimensional crystalline state because ideally a
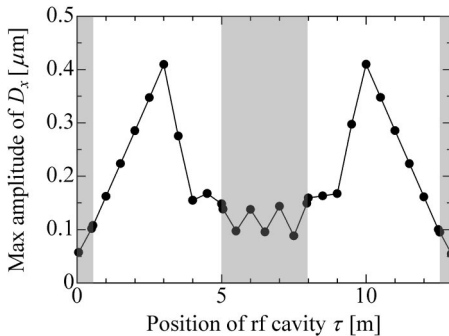
FIG. 6. Maximum amplitude of the horizontal orbit function D_x vs longitudinal position of an rf cavity. We have assumed exactly the same lattice parameters as used in Fig. 5. Six cooling sections have been inserted symmetrically, so that we can consider only a single lattice period in the picture. When the cavity is located within the shaded area in each period, D_x shows an oscillation pattern similar to that in Fig. 4. This result agrees fairly well with numerical simulations.
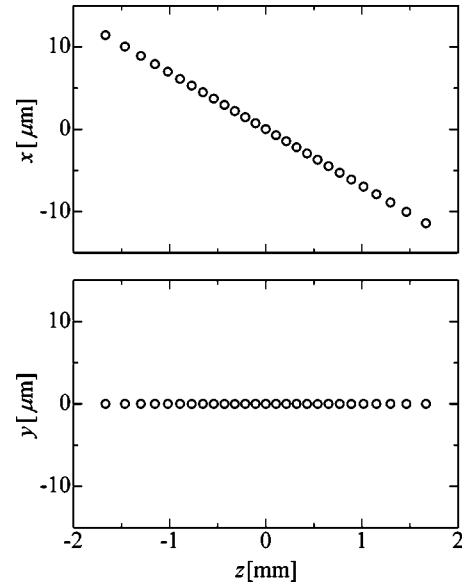
FIG. 7. Long-term stability of an oscillating Coulomb chain. Plotted is the spatial configuration of the crystalline beam in Fig. 1, 15 000 turns after the cooling was stopped.

coasting Coulomb chain is completely static in the rest frame. (This does not necessarily mean that we can, in practice, crystallize any low line-density beams.) It is, however, uncertain about whether a bunched Coulomb chain is as stable as coasting ones. Since it inevitably has a finite oscillation amplitude in the horizontal direction, transverse collective instabilities may be induced more seriously. It has actually been known that a multidimensional crystalline beam is unstable in a storage ring that does not satisfy the condition [7]

$$\max(\nu_x, \nu_y) < \frac{N_{sp}}{2\sqrt{2}}. \tag{13}$$

Though the case-I lattice meets this requirement because $N_{sp}=6$ and $(\nu_x, \nu_y)=(2.10, 2.10)$, we must remember that the longitudinal rf force substantially affects the transverse motion of a Coulomb chain. In the case of Fig. 1, for instance, the actual superperiodicity of the ring is one rather than six as is evident from the single-particle trajectories in Fig. 2; the condition (13) has thus been broken. If this oscillating Coulomb chain is really in a complete ground state, it should be stable even without the dissipative force. Figure 7 shows its spatial profile, 15 000 turns after the cooling effect was removed. We observe that the linear configuration is still maintained. The root-mean-squared (rms) emittances at this moment are 2.20×10^{-18} m rad in the horizontal direction and 2.95×10^{-15} m rad in the longitudinal direction, near the values 1.82×10^{-19} m rad and 2.87×10^{-15} m rad just before we stopped cooling.

It is also worthy to examine the stability of a bunched string in the case-II lattice where $(\nu_x, \nu_y)=(2.30, 2.30)$. In this case, the condition (13) never holds even after six cavities are symmetrically installed in the ring. We, however,
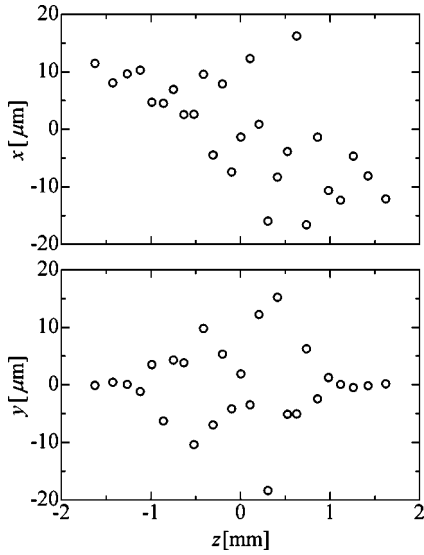
FIG. 8. Spatial configuration of a bunched beam cooled by the linear dissipative force with $f_x = f_y = 0.01$ and $f_z = 0.33$. Other parameters are identical to those in the case of Fig. 1.

FIG. 9. Threshold number of ions in a bunch and the corresponding plasma parameter vs bare synchrotron tune. The lattice parameters are identical to those in the case of Fig. 1.

found that the string motion is quite stable without the cooling force.

Another factor that crucially influences beam stability is the cooling force itself. Owing to dispersion, the average velocities of individual particles forming a crystalline beam are slightly different depending on their horizontal positions; in order for all particles to have an identical revolution frequency, a radially outer particle must travel faster than inner particles. This suggests that, at an ultralow temperature, simple dissipation as defined in Eq. (12) no longer operates as a cooling force but can rather cause a heating effect because it tries to equalize the longitudinal velocities of all particles. The usual laser-cooling force basically has the same defect. In the simulation of Fig. 1, we have considered a modest linear friction with $f_x = f_y = 0.01$ and $f_z = 0.11$, so that the dispersive heating is not too serious. If the longitudinal friction coefficient f_z is, for example, tripled, then the ordered structure is completely destroyed as demonstrated in Fig. 8. The normalized rms emittances are now roughly 10^{-13} m rad in all three directions, several orders of magnitude larger than the values in Fig. 1. We thus conclude that it is desirable to properly "taper" the laser cooling force in order to compensate the destructive dispersive effect [23].

It should be informative to mention the simulation results in which we considered one cavity and six cooling sections around the ring. In this case, we found it still possible to realize one-dimensional ordering. The ordered structure was, however, unstable; it was immediately melted away once the cooling force was removed. This should again be attributed to momentum dispersion.

C. Temperature, transition density, and oscillating zigzag

The behavior of a classical one-component plasma can be characterized by the Coulomb coupling parameter Γ defined by $\Gamma = (q^2/4\pi\varepsilon_0 \bar{d})/k_B T$, where $\bar{d}$ is the average interparticle
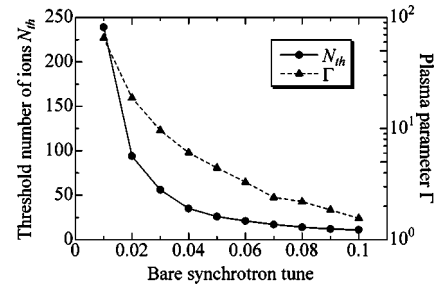
distance, k_B is the Boltzmann constant, and T is the thermodynamic temperature of the beam [24]. It is often said that the phase transition to a crystalline state takes place when Γ exceeds about 170 [25]. In an alternating-gradient focusing system, however, this statement is clearly irrelevant because the envelope of any multidimensional crystalline beam is forced to "breathe" periodically. Provided that the beam is bunched, even a one-dimensional crystal oscillates transversely as verified in previous sections. Further, the thermodynamic temperature of a three-dimensional crystal is expected to grow as the number of shells increases, while the value of $\bar{d}$ is roughly maintained. Consequently, the Γ value of a crystalline beam is generally much smaller than 170. For instance, the plasma parameter of the Coulomb chain in Fig. 1 is only 4.4. Since the transverse oscillation amplitude of a Coulomb chain depends on the rf voltage V_0, Γ is also V_0 dependent. One possible way to avoid this ambiguity of Γ is the use of the emittance concept. The rms emittance of an ideal crystalline beam is actually zero regardless of its spatial configuration [10]. It may thus be useful and convenient to redefine the threshold of phase transition on the basis of beam emittance.

The threshold number of ions, at which a string converts into a zigzag, is plotted in solid line in Fig. 9, while the broken line indicates the corresponding plasma parameter. The interparticle spacing $\bar{d}$ in this case was always over 100 μm, more than twice as large as the theoretical prediction for coasting crystalline beams [12]. We have also confirmed that the threshold depends not only on V_0 but also on the cooling strength; conversion to a zigzag crystal tends to occur at a smaller number of ions as the cooling force becomes weaker.

Finally, let us briefly look at the configuration of a bunched zigzag beam for reference. Since the oscillating Coulomb chain in Fig. 1 has the critical line density, we can transform it to the zigzag configuration simply by adding one more ion. Figure 10 shows the simulation result. Unlike a coasting zigzag beam, these 28 ions execute betatron oscillations, passing by each other in the vertical direction. They also oscillate horizontally just like in the case of a bunched string. These systematic oscillations of particles have made the beam temperature even higher than the level of bunched Coulomb chains; it is over 0.5 K, two orders of magnitudes greater than the Doppler limit of laser cooling. Similar to the case of one-dimensional crystalline beams, the oscillation
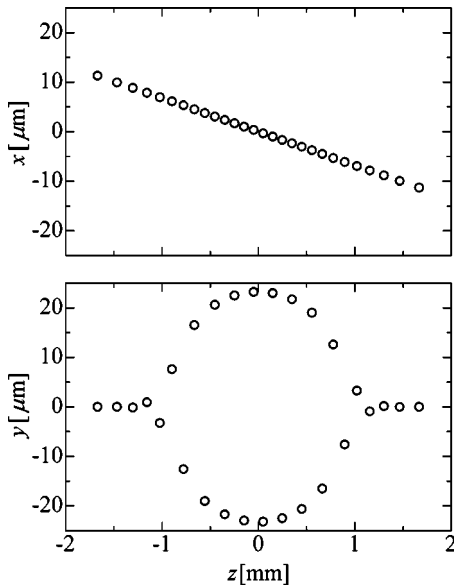
FIG. 10. Spatial configuration of a bunched zigzag crystalline beam obtained from a multiparticle simulation. The lattice parameters are identical to those in the case of Fig. 1.

pattern of each particle depends on the details of the lattice structure.

V. CONCLUDING REMARKS

In this paper, we theoretically investigated the dynamic properties of one-dimensional crystalline beams under the influence of a longitudinal rf potential. It was demonstrated that, unlike a coasting string, a bunched string in a storage ring shows unique features due to the existence of momen-

tum dispersion. Systematic numerical simulations revealed that the periodic oscillatory motion of a Coulomb chain is quite sensitive to the lattice design such as the number and positions of rf cavities. To predict the oscillation pattern in an arbitrary ring, we derived approximate equations of string motion making some fundamental assumptions. It was confirmed that the stationary solution to Eqs. (10) and (11) can well reproduce the complex motion of an oscillating Coulomb chain.

Bunched one-dimensional crystals turned out to be stable even without the maintenance condition (13) satisfied. The present results, however, suggest that it is essential to minimize the heating effect caused by momentum dispersion. The best way to suppress the dispersive instability is the use of a tapered cooling force although how to develop such a special force is a future issue.

One possible scenario for the production of a string crystalline beam may be as follows: At high temperature and/or low line density, the longitudinal laser-cooling force does not affect the transverse betatron motion because the natural Coulomb coupling among stored ions is negligible. We, therefore, first employ the *resonant coupling method* to artificially improve the transverse cooling efficiency [26]. Since a synchrobetatron resonance is used in this three-dimensional cooling scheme, the beam must be bunched at the beginning [27]. After the beam has reached an ultracold equilibrium state, we adiabatically reduce the rf voltage or laser power (or both) to weaken the dispersive heating. If the lattice design is proper, we will then observe an anomalous beam response similar to those in the electron-cooling experiments at NAP-M, ESR, and CRYRING. Considering the fact that the Doppler limit is much lower than the temperature of currently available cold electron beams, the final state can be a Coulomb crystal.

[1] S. Schröder *et al.*, Phys. Rev. Lett. **64**, 2901 (1990).
[2] J.S. Hangst *et al.*, Phys. Rev. Lett. **67**, 1238 (1991).
[3] See, e.g., *Crystalline Beams and Related Issues*, edited by D. M. Maletic and A. G. Ruggiero (World Scientific, Singapore, 1996).
[4] J.P. Schiffer and P. Kienle, Z. Phys. A **321**, 181 (1985); A. Rahman and J.P. Schiffer, Phys. Rev. Lett. **57**, 1133 (1986).
[5] J. Wei, X.-P. Li, and A.M. Sessler, Phys. Rev. Lett. **73**, 3089 (1994).
[6] H.-J. Miesner *et al.*, Phys. Rev. Lett. **77**, 623 (1996).
[7] J. Wei, H. Okamoto, and A.M. Sessler, Phys. Rev. Lett. **80**, 2606 (1998).
[8] T. Kihara *et al.*, Phys. Rev. E **59**, 3594 (1999).
[9] N. Madsen *et al.*, Phys. Rev. Lett. **83**, 4301 (1999).
[10] H. Okamoto, Phys. Plasmas **9**, 322 (2002).
[11] T. Schätz, U. Schramm, and D. Habs, Nature (London) **412**, 717 (2002); U. Schramm, T. Schätz, and D. Habs, Phys. Rev. Lett. **87**, 184801 (2001).
[12] R. Hasse and J.P. Schiffer, Ann. Phys. (N.Y.) **203**, 419 (1990).
[13] H. Okamoto and J. Wei, Phys. Rev. E **58**, 3817 (1998).
[14] K. Okabe and H. Okamoto, Jpn. J. Appl. Phys. (to be published).

[15] A lower heating rate means less intraparticle collisions. At low line density, therefore, we can no longer rely on the sympathetic effect for transverse cooling.
[16] V.V. Parkhomchuk and N.S. Dikansky, Sov. J. Tech. Phys. **50**, 1411 (1980); E.N. Dementev *et al.*, Sov. Phys. Tech. Phys. **25**, 1001 (1980).
[17] M. Steck *et al.*, Phys. Rev. Lett. **77**, 3803 (1996).
[18] H. Danared *et al.*, Phys. Rev. Lett. **88**, 174801 (2002).
[19] R.W. Hasse, Phys. Rev. Lett. **83**, 3430 (1999).
[20] Y. Yuri and H. Okamoto, J. Phys. Soc. Jpn. **71**, 1003 (2002).
[21] J. Wei, X.-P. Li, and A. M. Sessler, Brookhaven National Laboratory Report No. BNL-52381, 1993 (unpublished).
[22] T. Katayama *et al.*, in *Proceedings of the 2nd European Particle Accelerator Conference*, edited by P. Martin and P. Mandrillon (Editions Frontiéres, Gif-sur-Yvette, 1990), p. 577.
[23] Note, however, that the amount of optimum tapering is a function of the longitudinal coordinate τ and lattice dependent. Since a laser-cooling region generally extends over a sufficiently long straight section of a ring, we can only match the tapering factor in an average sense.
[24] S. Ichimaru, Rev. Mod. Phys. **54**, 1017 (1982).
[25] W.L. Slattery, G.D. Doolen, and H.E. DeWitt, Phys. Rev. A **21**, 2087 (1980).

[26] H. Okamoto, A.M. Sessler, and D. Mohl, Phys. Rev. Lett. **72**, 3977 (1994); H. Okamoto, Phys. Rev. E **50**, 4982 (1994).

[27] Laser cooling of a bunched beam has some practical merits compared to that of a coasting beam. For instance, it naturally provides stable fixed points in the longitudinal phase-space plane, which counteracts diffusive heating such as intrabeam scattering; see, e. g., J.S. Hangst *et al.*, Phys. Rev. Lett. **74**, 4432 (1995).